PHYSICSAccess Research Paper
ISSN Online: 2756-3898, ISSN Print: 2714-500X https://doi.org/10.47514/phyaccess.2023.3.1.002

Structural and Electronic Properties of Cu^{2+} Doped $LiMn_2O_4$ Cathode Material for Rechargeable Lithium Ion Battery: A DFT Study

Owolabi J Adeyemi[1], Muhammad Y Onimisi[1], Victor A Odoh[1], Hassan G Muhammad[1] and Mohammad L Madugu[2]

[1] Department of Physics, Nigerian Defence Academy, Kaduna, Kaduna State, Nigeria
[2] Department of Physics, Faculty of Science, Gombe State University, Gombe State, Nigeria

Corresponding E-mail: alogaodoh@nda.edu.ng

Received 17-12-2022
Accepted for publication 27-02-2023
Published 01-03-2023

Abstract

Spinel $LiMn_2O_4$ offers a potentially attractive alternative to the commercialized $LiCoO_2$ because of its low cost, non-toxicity, good rate performance and superior safety, but experiences severe capacity fading as a result of Jahn-Teller cubic phase transition to unstable tetragonal phase especially when operated at elevated temperature (>55ºC). Among the various techniques carried out to overcome these setbacks is doping with cations to raise the oxidation state of Mn thereby decreasing the amount of unstable Mn^{3+}. This study focuses on the investigation of the structural and electronic properties of Cu^{2+} doped $LiMn_2O_4$ using ab-initio computational method. The structural properties of both un-doped $LiMn_2O_4$ and Cu_{2+} doped $LiMn_2O_4$ were collectively obtained using both generalized gradient approximation (GGA) employing pseudo-potentials, plane wave basis sets and XcryDen. From the electronic properties of undoped $LiMn_2O_4$, it was revealed that in $LiMn_2O_4$, only Mn^{3+} ions contribute to conduction, even though Mn^{3+} ions and Mn^{4+} ions exist together. Increasing the number of Mn^{3+} brings it a unique challenge of instability. Due to this instability, avoiding the Mn^{3+} state of manganese prevents Jahn-teller distortion, resulting in a reduced phase transition. Based on the results from the first-principles calculation of Cu^{2+} doped $LiMn_2O_4$, the Cu valence in doped spinel $LiCu_{0.25}Mn_{0.75}O_4$ is Cu^{2+} at a fully lithiated state. When half of the Li ions are extracted, the Cu^{2+} ions oxidized to Cu^{3+} ions. Since Cu^{2+} is a di-valent element, the dopant act as electrochemically active centres for valence change, leaving two trivalent ions to only take on +4 oxidation states stably, thus increasing Mn-O bonding strength which ultimately suppressed Jahn-Teller distortions. However, previous studies show that Cu^{2+} substitution shrinks the lattice because the ionic radius of Cu^{2+} is smaller than that of the host Mn^{3+} ions, thereby the reversible capacity of Cu-doped spinel may be reduced as Cu ions can only provide one electron per ion.

Keywords: Cathode material; Density of state; Band structure; Cation doping; Density Functional Theory.

I. INTRODUCTION

Electricity has been a necessity for humanity ever since it was founded, but today's global energy crisis and environmental pollution have made it necessary for people to switch from traditional energy sources to renewable ones like solar, wind, geothermal, and tidal energy. These renewable energy sources are often gathered as electrical energy before being distributed to consumers. However, a common issue with many renewable energy sources is how little electrical energy can be stored. Although it can be stored directly thanks to capacitors, the available supply is minimal compared to the demand for most applications [1]. Typically, electrical energy must be converted into another form of energy before being stored, therefore the choice of an energy storage technology is crucial.

One of the most popular technologies that can convert electrical energy back into chemical energy for storage and continuously provide clean power for use is the use of rechargeable (secondary) lithium batteries. The main benefit of employing lithium-ion battery technology for energy storage is that lithium is the lightest and most electropositive metallic element, which makes it possible to have very high energy densities while being environmentally friendly [2]. The development of wireless and portable electronic devices was made possible by lithium-ion battery technology, which also rekindled the search for batteries to power electric and hybrid automobiles.

Lithium cobalt oxide ($LiCoO_2$) was used as the cathode in the initial generation of lithium-ion batteries; however, this substance is both expensive and hazardous. Lithium manganite systems appear to offer a workable solution to the issues as a result of research to identify an alternate material. A prospective replacement for currently available lithium rechargeable battery cathode materials based on nickel and cobalt oxides is the lithium manganese oxide spinel ($LiMn_2O_4$).

$LiMn_2O_4$, a lithium manganate with a spinel structure, has long been known to intercalate lithium. It has been extensively investigated as a positive electrode due to its exceptional electrochemical activity, low cost, relative cost abundance, environmental friendliness, stability, and high columbic efficiency. It also has a high potential of 3.0-4.5 V, excellent rate capability from its 3-D framework structure, and high columbic efficiency.

However, its severe capacity fading caused by the structural phase transition from a stable cubic phase to an unstable tetragonal phase as a result of the Mn^{3+} ions' Jahn-Teller distortion, disproportion reactions, and surface reactions with acidic contaminants in the electrolyte, especially at elevated temperature, severely restricts its full industrial application in the highly competitive energy storage market [3].

Doping with cations to replace a portion of Mn^{3+} ions at 16d sites to raise the oxidation state of Mn and thereby reduce the amount of unstable Mn^{+3} is one method used to overcome these obstacles. Doping is an efficient way to suppress the Jahn-Teller distortion and to improve the cycling performance of $LiMn_2O_4$ [4].

The typical method of material exploration and research follows the synthesis-structure-property thread, and interpretations are frequently based on straightforward experimental observation and analysis. Typically, this procedure takes too long and is ineffective. A more effective and economical method has been created for forecasting and analysing material structures as a result of advances in computing technologies and sophisticated theoretical techniques using the Density Functional Theory (DFT) [5].

All calculations of systems at the atomic level, whether they are calculations to establish the atomic structure of a material or calculations to determine it's electronic, optical, or other physical properties, begin with the fundamental laws of quantum mechanics. The actual unresolved problem in quantum mechanics is how to deal with indistinguishable, interacting particles, notably electrons. Density functional theory (DFT) is a ground-state theory that emphasizes charge density as the relevant physical parameter and may be successfully used to compute various ground state properties of various systems. Theoretically, the DFT can calculate any attribute that can be obtained by resolving Schrödinger's equation. It is possible to quickly screen the impact of various doping elements on the electrical structure of $LiMn_2O_4$ using the first principle DFT computational modelling [6].

Several investigations have been conducted to improve and stabilize the structural characteristics of $LiMn_2O_4$ by lowering the Mn^{3+} concentration and stabilising the cubic structure from the Jahn-Teller distortion effect [7].

By doping $LiMn_2O_4$ with the Cu^{2+} cation, this work attempts to identify and improve the material's structural and electrical properties by increasing its conductivity period. The Jahn-Teller phase transition is predicted to be suppressed by the replacement of Mn ions with Cu^{2+} because it will increase the average oxidation state of Mn and reduce the number of unstable Mn^{3+}. Due to its better electronic conductivity, capacity to decrease the activation barrier for Li diffusion in spinel, capacity to participate in the charge transport process, and ability to be more stable during electrochemical cycling, Cu^{2+} was chosen for this study's dopant.

II. COMPUTATIONAL METHOD

The Perdew-Burke-Ernzerhof generalized gradient approximation (PBE-GGA) pseudo potential has been utilized to approximate the exchange-correlation potential for both doped and undoped $LiMn_2O_4$ in all computations performed in this study using the Quantum-ESPRESSO code. For integrals, the Maxfessel-Paxton smearing approach was used.

Brillouin zone sampling (k-points) was carried out with an increment of $2 \times 2 \times 2$ in the range from $2 \times 2 \times 2$ to $10 \times 10 \times 10$, by fixing the other parameters constant. The values of minimum energies obtained to the corresponding k-point grids were plotted and a $(6 \times 6 \times 6)$ mesh of Monkhorst-pack special k-points was selected for this project since the

structure was well converged at this k-points mesh. Also, the convergence test for total minimum energy as a function of cut-off energy (e_{cutwfc}) is performed with an increment of 10 Ry in the range of 20 to 60 Ry. The optimized value for plane wave cut-off of 40 Ry was used for all calculations.

To ensure accuracy in this study k-point of $6 \times 6 \times 6$ and cut-off energy (e_{cutwfc}) of 40 Ry were used to create an input file for the subsequent calculations.

Doping was done by the substitution of the Mn atom by Cu^{2+} dopants at the $(0.12500: 0.12500: 0.12500)$ positions. The four manganese atoms were replaced by one copper ion making a 25% occupancy by the dopant.

III. Results and Discussion

A. Total energy convergence test results and discussion

The self-consistency energy convergence threshold ($conv_{thr}$), the Brillouin zone sampling k-points and the plane wave kinetic energy cut-off (E_{cutwfc}) for the material of interest are all necessary for accurate DFT calculations. The aforementioned parameters were optimized with energy reduction to acquire the right results in this work.

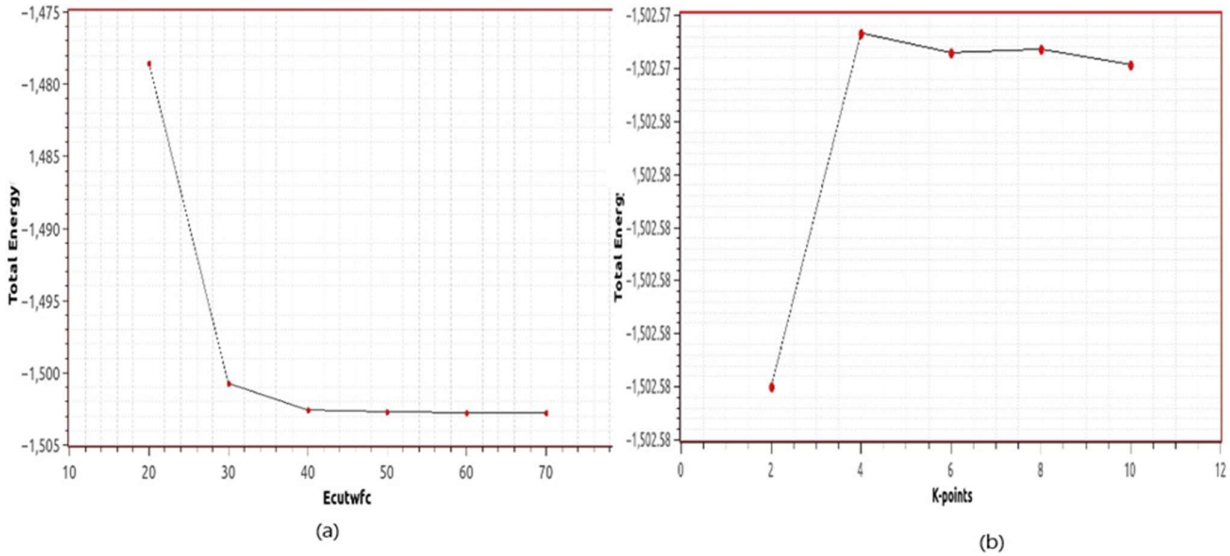

Fig. 1 (a) convergence of the total energy of $LiMn_2O_4$ to the kinetic energy cut-off (E_{cut}) (b) convergence of the total energy of $LiMn_2O_4$ to the k-point grid

Plane-wave self-consistent field (PW_{scf}) calculations are based on convergence tests to plane-wave energy cut-off and k-point mesh. Fig. 1(a) illustrates the convergence of the total energy of $LiMn_2O_4$ to the kinetic energy cut-off (E_{cut}). With an increment of 10 Ry between 20 and 70 Ry, the convergence test for total minimum energy as a function of cut-off energy is conducted. The remaining input file characteristics are fixed while the energy cut-off is varied.

The convergence of the $LiMn_2O_4$'s total energy to the k-point grids is depicted in Fig. 1(b). By holding the other parameters constant, the convergence test for the total minimum energy vs. k-point sampling with an increment of $2 \times 2 \times 2 \times 2$ is carried out. The total energy E_{tot} (eV) changes significantly, as shown in Fig. 1(b), but there is some stability between the grid sizes ($6 \times 6 \times 6$ and $10 \times 10 \times 10$), which results in less significant changes in total energy. For this reason, the $6 \times 6 \times 6$ grid is chosen as the optimal k-point value.

B. Un-doped Structural and Electronic Properties

Fig. 2 shows that the stable phase of undoped $LiMn_2O_4$ crystallizes in the cubic Fd3m space group at room temperature. In this cubic structure, manganese ions occupy the octahedral positions (16d), oxygen ions occupy the tetrahedral positions (32e), and lithium ions occupy the tetrahedral (8a) positions. Each of them has voids separating it from four nearby ions (16c). The remaining vacant spaces are connected and provide a 3D diffusion channel for the quick diffusion of lithium ions. The three-dimensional MO_2 host serves as the structure's foundation, and the transition metal layer's vacancies guarantee the three-dimensional Li diffusion paths.

Another finding in the structure mentioned above is that all of the atoms in the spinel $LiMn_2O_4$ structure are linked by strong chemical bonds that run across the lattice, making it simple for Li to intercalate or de-intercalate into the structure. Each 8a tetrahedron shares all four of its faces with a 16c

octahedral unit, which is a significant characteristic of this cubic spinel structure.

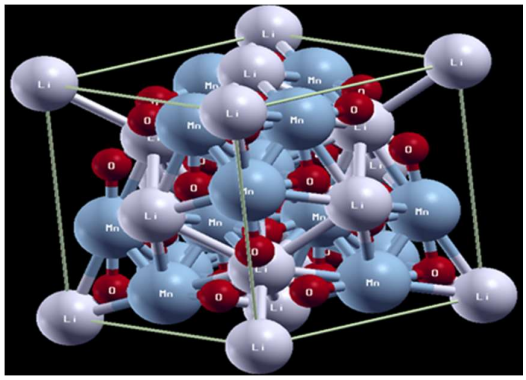

Fig. 2 Structure of Un-doped LiMn2O4 using XcryDen.

C. Density of state (DOS) of Un-doped $LiMn_2O_4$.

The electronic structure of undoped $LiMn_2O_4$ is examined in this section using the density of state (DOS). Fig. 3 and 4 display, respectively, the DOS of $LiMn_2O_4$, Li ions, Mn ions, and O ions. While the lithium atoms in the spinel structure are significantly ionized, the electronic structure of $LiMn_2O_4$ is controlled by a strong hybridization between the Mn-d and the O-p states.

With an equal amount of anti-ferromagnetic aligned Mn^{3+} and Mn^{4+} ions, the average valence of Mn ions is +3.5. The d orbitals split into two E_g orbitals as a result of the Mn ions in the O octahedral sites. Because there is a band gap betweent_{2g} and e_g and three valence electrons filling three t_{2g} orbitals while leaving one unfilled in Mn^{4+}, the ion acts as an insulator.

According to Fig. 4, the 3d states of Mn atoms contributed to the first peak in the valence band, which is dominated by these states along with some contributions from the 3p states of O atoms and the 2s states of Li. There are no maximum peaks in the conduction band; instead, the shallow peaks just before the Fermi energy are dominant. These peaks come from the 3p orbitals of oxygen and are dominated by three broad peaks.

Thus, from this research, even though Mn^{3+} ions and Mn^{4+} ions coexist in $LiMn_2O_4$, only Mn^{3+} ions contribute to conduction. But as the Mn^{3+} content rises, instability poses a special problem. This instability causes Jahn-teller distortion to be prevented by the manganese in the Mn^{3+} state, which reduces phase transition.

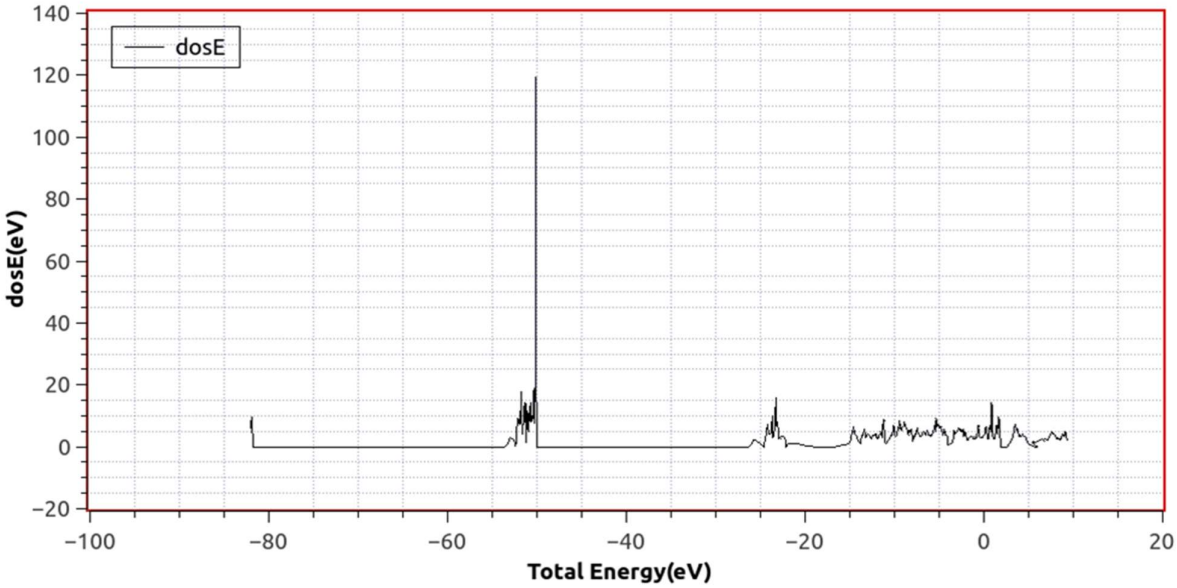

Fig. 3 The density of state of Un-doped $LiMn_2O_4$

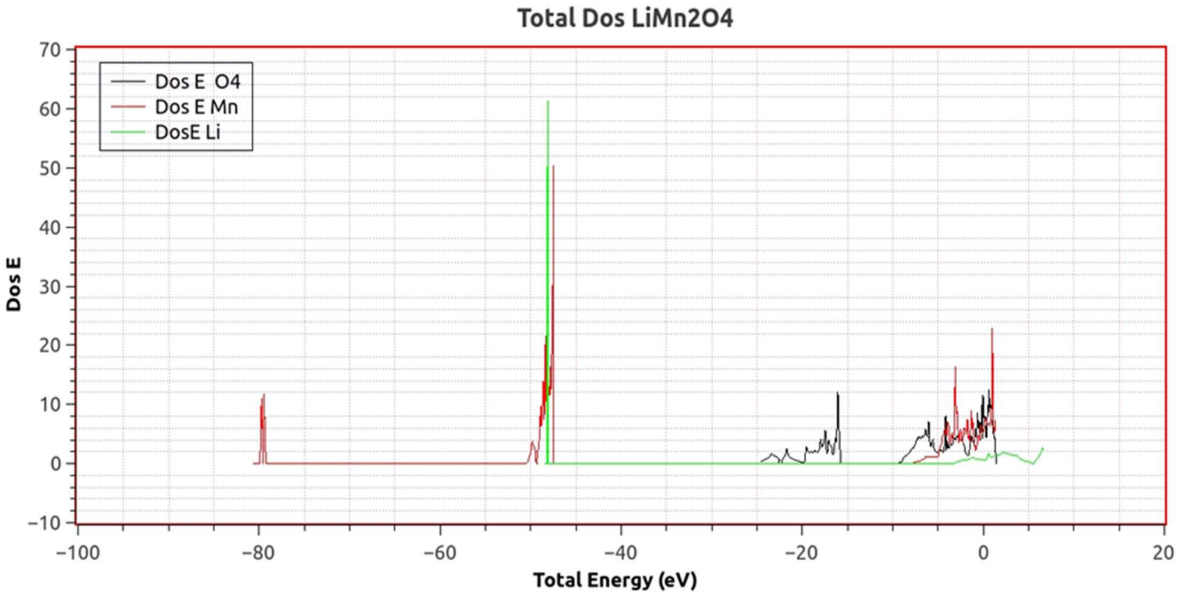

Fig. 4 Partial Density of State of Un-doped $LiMn_2O_4$ indicating the number of states per atom.

D. Band Structure of Un-doped $LiMn_2O_4$

The calculated electronic band structures of Un-doped $LiMn_2O_4$ are shown in Fig. 5, using pbe-GGA, the bands were selected along 6 symmetry points which are ($\Gamma \rightarrow X \rightarrow$ K $\rightarrow$ L $\rightarrow X \rightarrow \Gamma$) and the band structure energy range is plotted from 0.0 eV to 15.0 eV. The red line represents Fermi Level. LiMn2O4 is considered a semiconductor based on the above calculation of its band structure. Also, as seen from Fig. 5, at Γ point, the presence of the valence band and conduction band around different symmetry points. This indicates that the materials have indirect band-gap nature.

The resulting electronic band structure resulting from the calculation exhibits a small band gap of 4.3 eV, in agreement with previous studies using similar parameters [8].

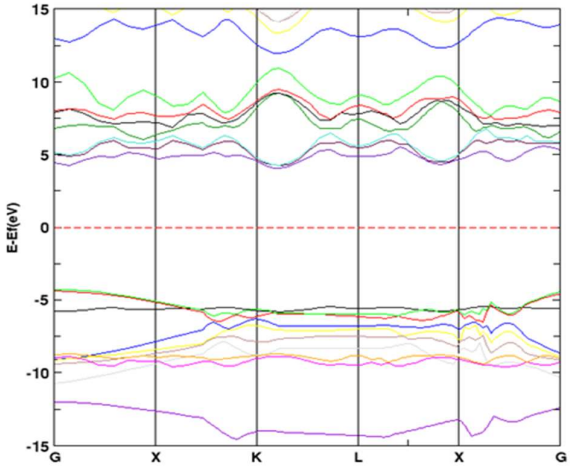

Fig. 5 Calculated band structures of the undoped $LiMn_2O_4$

E. Structural and electronic properties of Cu^{2+} Doped $LiMn_2O_4$

The schematic primitive diagram of the Cu^{2+} doped $LiMn_2O_4$ lattice atom group is shown in Fig. 6. The face-centre cubic lattice makes up each of the two lithium, three manganese, one copper, and eight oxygen atoms that make up the structure of Cu^{2+} doped $LiMn_2O_4$.

The cubic spinel $LiMn_2O_4$ has a cation distribution of (Li)8a (Mn_2)16d O_4 as seen in Fig. 6, the subscripts 8a and 16d denote Fd3m symmetric cation sites. Tetrahedral 8a sites are occupied by Li ions, while the octahedral 16d sites are occupied by Mn ions. The O ions at the 32e sites form a cubic closest packed (ccp) structure.

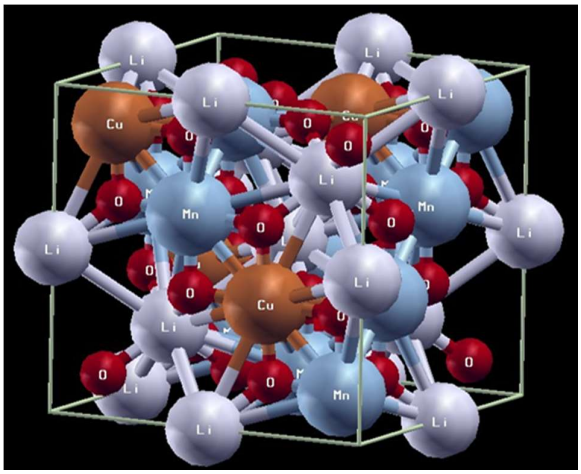

Fig. 6 Structure of Cu2+ doped $LiMn_2O_4$ using XcryDen.

Mn ions have an average valence state of +3.5, whereas Li and O ions have valence levels of +1 and -2, respectively. At the 16d octahedral location, some of the Mn ions are swapped out for Cu^{2+} ions, creating a solid solution with the chemical formula $LiCu_{0.25}Mn_{1.75}O_4$.

F. Density of state (DOS) of Cu^{2+} doped $LiMn_2O_4$

The Density of State of Cu $^{2+}$ doped $LiMn_2O_4$ is shown in Fig. 7 the highest peak in the valence band denotes contributions from the Mn atom's 3d states.

In the conduction band, the Mn-4d orbitals form the small, high peak immediately after the Fermi energy, and the visible shallow peaks are states derived from a combination of Mn-3d, Cu-1s, and O-2p orbitals. The sharp peaks just before the Fermi energy originates from the Cu-3d orbitals.

Fig. 8 and 9, which exhibit the partial density of state of the dope $LiCu_{0.25}Mn_{1.75}O_4$ and the partial density of state of the doped $LiCu_{0.50}Mn_{1.50}O_4$ respectively, demonstrate the number of states per atom.

Li^+ ions, Mn^{3+} ions, and Mn^{4+} ions are the three main forms of cations found in $LiMn_2O_4$. In Fig. 8, a 25 per cent Cu doping was performed. It can be seen that the first and highest peak results from a Mn-1s state, followed by a Mn-3p state and a Cu-3d state just before the Fermi energy, and the conduction band. From the observation that Mn-3p results in the highest peak at the conduction band, it can be inferred that Cu ions occupy 4b octahedral sites and Li ions.

The highest peak in Fig. 9, which has more Cu doping, is caused by the Mn-3p state; in contrast to Fig. 7, which clearly shows that there are more Mn^{4+} ions than Mn^{3+} ions, Li ions are more likely to be surrounded by Mn^{4+} ions. Due to the electrostatic effect, combining Li^+ and Mn^{4+} ions can limit the localization of positive charges and further lower the system's overall energy.

As a result, Mn^{4+} ions have less dense electron clouds than Mn^{3+} ions, which results in weaker Mn-O interactions and longer Mn-O bond lengths. These shorter Li-O bond lengths then result in smaller Li 16c site octahedral volumes. Due to the stronger Coulombic repulsion between Li^+-Mn^{4+} and Li^+-Mn^{3+}, the Li^+-Mn^{4+} distances are longer than Li^+-Mn^{3+} distances [9]. When the electrostatic balance is reached, the Li-Mn^{3+}/Mn^{4+} distances spread with wide distribution, reducing the elongation or contraction of the Mn-O bond pointing towards vertex O as a result of the asymmetric shape of d electron

These first-principles calculations' findings indicate that the Cu valence in the doped spinel $LiCu_{0.25}Mn_{0.75}O_4$ is Cu^{2+} in the fully lithiated state. The Cu^{2+} ions oxidized to Cu^{3+} ions upon extraction of half of the Li ions. However, because Cu ions can only supply one electron per ion, the reversible capacity of Cu-doped spinel may be diminished. But it is possible to lower the Li diffusion activation barriers when doped with a small amount of Cu, as in Fig. 8, to achieve a higher rate capability.

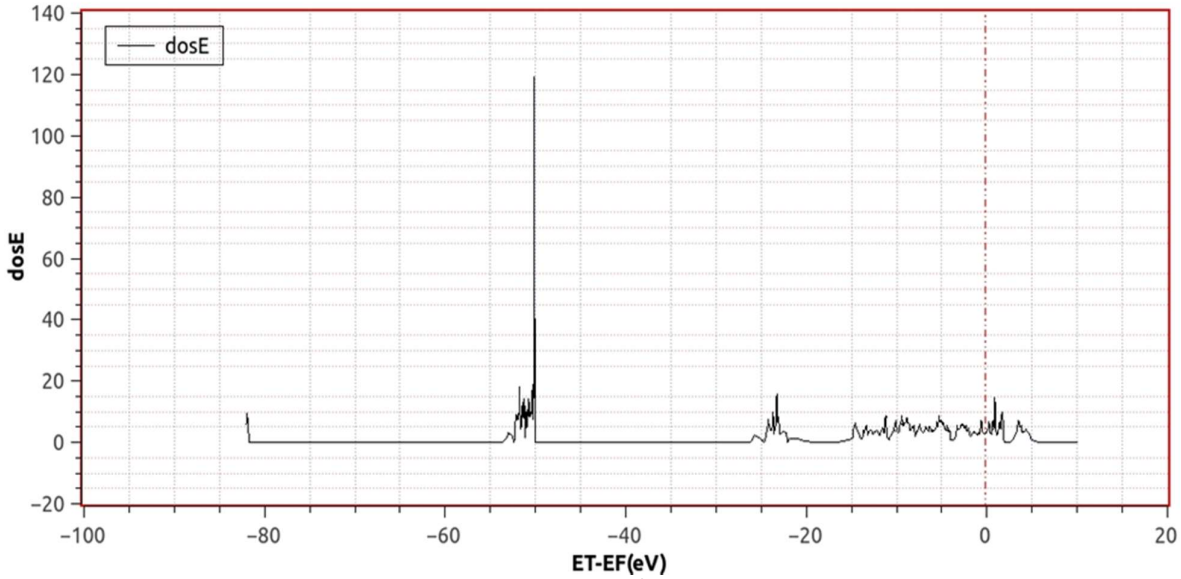

Fig. 7 Density of State of Cu^{2+} dope $LiMn_2O_4$

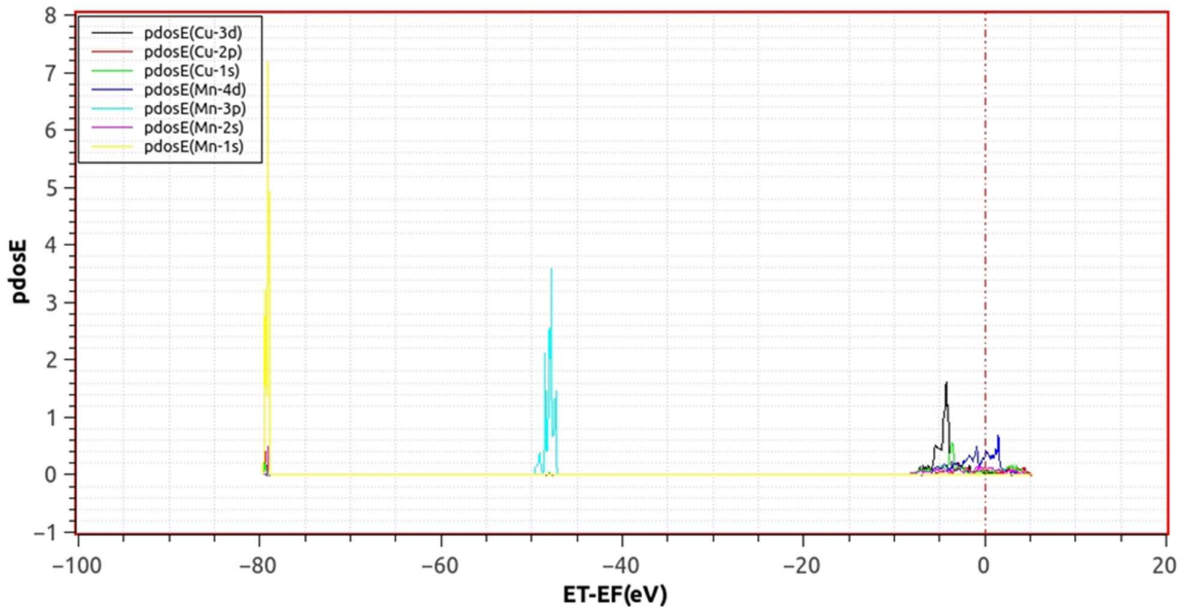

Fig. 8 Partial Density of State of dope $LiCu_{0.25}Mn_{1.75}O_4$ indicating the number of states per atom

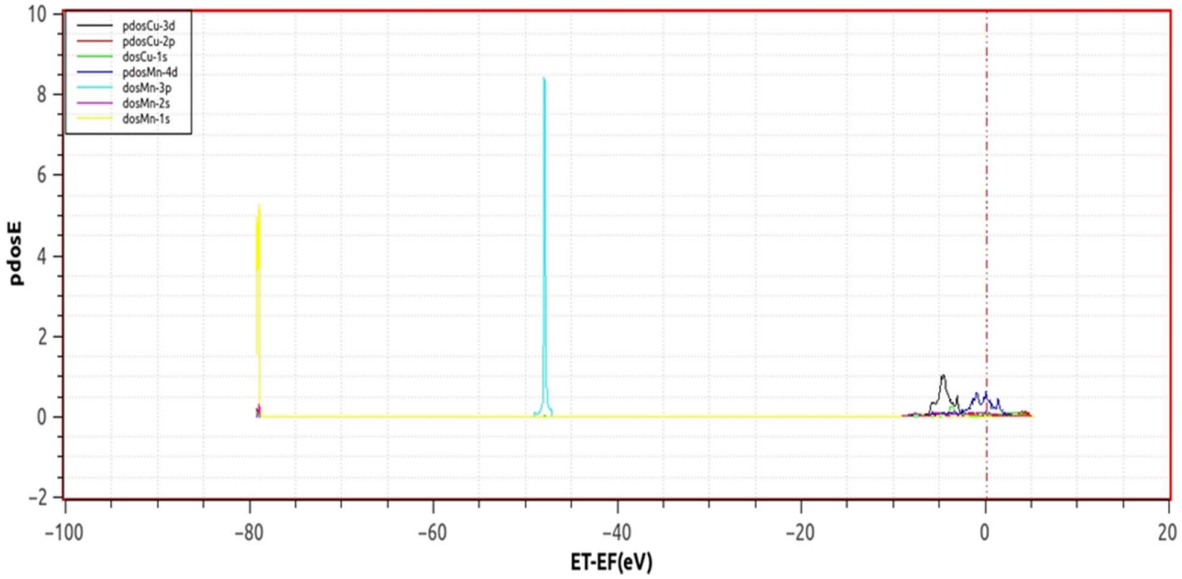

Fig. 9 Partial Density of State of dope $LiCu_{0.50}Mn_{1.50}O_4$ indicating the number of states per atom

G. Band Structure of doped $LiMn_2O_4$

Fig. 10 shows the calculated electronic band structures of doped $LiCu_{0.25}Mn_{1.75}O_4$ the bands were selected along 6 symmetry points which are ($\Gamma \rightarrow X \rightarrow \mathrm{K} \rightarrow \mathrm{L} \rightarrow \rightarrow \Gamma$) and the band structure energy range is plotted from $0.0\ eV$ to $15.0\ eV$. The red line represents Fermi Level. Based on the above calculation of band structure, $LiMn_2O_4$ is considered a semiconductor. Also, it shows the presence of the valence band and conduction band at around different symmetry points which indicates that the materials have indirect band gap nature.

The estimated results are consistent with some experimental data since the resulting electronic band structure has a wide valence bands width (VB) of $6.90\ eV$ and a small conduction bandwidth (CB) of $2.24\ eV$. The electronic band structure calculated here is fairly similar to the reported values of $1.923\ eV$ [10].

Cu^{2+} is a divalent element, so the dopant functions as electrochemically active centres for valence change, leaving only two trivalent ions to take on stable +4 oxidation states. This increased the strength of the Mn-O bond, which in turn reduced Jahn-Teller distortions. Cu^{2+} substitution, however, causes the lattice to contract because its ionic radius is less than that of the host Mn^{3+} ions [4].

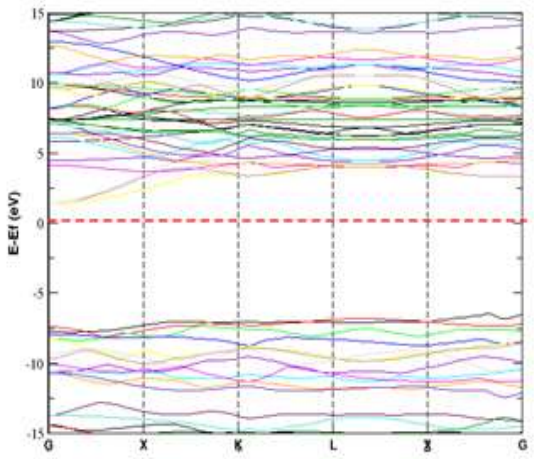

Fig. 10 Calculated band structures of the doped $LiMn_2O_4$

IV. Conclusion

Numerous significant electronic parameters, including band gaps and density of states, have been measured for both undoped and Cu^{2+} doped $LiMn_2O_4$ and results compared with theoretical and experimental findings. Though Mn^{3+} ions and Mn^{4+} ions coexist in $LiMn_2O_4$, it was discovered from the electrical characteristics of undoped $LiMn_2O_4$ that only Mn^{3+} ions contribute to conduction in this material. However as the Mn^{3+} content rises, instability poses a special problem. Due to its instability, avoiding the manganese's Mn^{3+} state is necessary to avoid Jahn-Teller distortion and a shortened phase transition. The Cu valence in doped spinel $LiCu_{0.25}Mn_{0.75}O_4$ is Cu^{2+} in a fully lithiated state, according to the findings of a first-principles calculation of Cu^{2+} doped $LiMn_2O_4$. After removing half of the Li ions, The Cu^{2+} ions oxidized to produce Cu^{3+} ions. Cu^{2+} is a divalent element, so the dopant functions as electrochemically active centres for valence change, leaving only two trivalent ions to take on stable +4 oxidation states. This increased the strength of the Mn-O bond, which in turn reduced Jahn Teller distortions. However, Cu^{2+} substitution causes the lattice to contract because the ionic radius of Cu^{2+} is smaller than that of the host Mn^{3+} ions. As Cu ions can only provide one electron per ion, this may reduce the reversible capacity of Cu-doped spinel.

References

[1] B. O. Jurgen, "*Handbook of battery materials"*. John Wiley and sons Inc. New York, 1999.

[2] O. Kazunori, "Lithium Ion Rechargeable Batteries". WILEY-VCH Verlag GmbH & Co. KGaA, Weinheim, 2009.

[3] L. Thamos, K, Raveendramat, R. M. Tomy, N. A George, S Jayalekshmi and J. Ravi, "Evidence of structure modification due to Jahn-Teller distortion in $Li_xMn_2O_4$ by photoacoustic spectroscopy. J Phy. D: App. Phy., vol. 40, no. 12, pp. 3807, 2007.

[4] J. Piao, S. Duan, X. Lin, X. Tao, Y. Xu, A. Cao and L. Wan, "*Surface Zn doped LiMn2O4 for an improved high temperature Performance"*. Chem. Comm., no. 42, pp. 5251-5390, 2018.

[5] Z. Tianran, L. Daixin, and T. Zhanliang, "Understanding electrode materials of rechargeable lithium batteries via DFT calculations". Prog. in Nat. Sci.: Mat. Inter., vol. 23, no. 3, pp. 256–272, 2013.

[6] Y. Li, "First-principles Calculations on the Electronic, Vibrational, and Optical Properties of Semiconductor Nanowires". Ph.D. dissertation, Sch. of Phy., Georgia Inst. of Tech., Georgia, 2006.

[7] K. Murali, T. Saravanan, and M. Jayachandran, "*Synthesis and characterization of copper substituted lithium manganate spinels"*. J Mat. Sci: Mat. Elect, vol. 19, pp. 533–537, 2007.

[8] D. Santos-Carballal, P.E. Ngoepe and N. H. de Leeuw, "Ab initio investigation of the thermodynamics of cation distribution and of the electronic and magnetic structures in the $LiMn_2O_4$ spinel," Phy. Rev. B, vol. 97, no. 8, pp. 085126-1 - 085126-11, 2018.

[9] A. Karim, S. Fosse and K.A. Persson, "Surface structure and equilibrium particle shape of the $LiMn_2O_4$ spinel from first-principles calculations," Phy. Rev. B, vol. 87, no. 7, pp. 075322-1 - 075322-6, 2013.

[10] G. Singh, S. L. Gupta, R. Prasad, S. Auluck, R. Gupta and A. Sil, "Suppression of Jahn–Teller distortion by chromium and magnesium doping in spinel LiMn2O4: A first- principles study using GGA and GGA+U". J. Phy. Chem., Solids, vol. 70, pp. 1200-1206, 2009).